



Evidence for Mogi doughnut behavior in seismicity preceding small earthquakes in southern California

Peter M. Shearer¹ and Guoqing Lin^{2,3}

Received 4 August 2008; revised 7 November 2008; accepted 26 November 2008; published 30 January 2009.

[1] We examine the average space-time behavior of seismicity preceding M 2–5 earthquakes in southern California from 1981 to 2005 using a high-resolution catalog and identify regions of enhanced activity in a 1-day period preceding larger earthquakes at distances comparable to their predicted source radii. The difference in precursory behavior between large and small earthquakes is subtle but statistically significant when averaged over many earthquakes, and it has similarities to the “Mogi doughnut” seismicity pattern observed to occur prior to some M 6 and larger earthquakes. These results indicate that many standard earthquake triggering models do not account for all of the processes involved in earthquake occurrence.

Citation: Shearer, P. M., and G. Lin (2009), Evidence for Mogi doughnut behavior in seismicity preceding small earthquakes in southern California, *J. Geophys. Res.*, 114, B01318, doi:10.1029/2008JB005982.

1. Introduction

[2] Earthquakes cluster strongly in time and space, but it is not yet clear how much of this clustering can be explained as triggering from previous events (such as occurs for aftershock sequences following large earthquakes) and how much the clustering may reflect underlying physical processes (such as apparently drive many earthquake swarms [e.g., Hainzl, 2004; Vidale and Shearer, 2006]). Seismologists have long studied the seismicity preceding big earthquakes to see if any distinctive precursory patterns could be identified. In some cases, a period of low earthquake activity or quiescence is observed for years in the vicinity of the eventual rupture zone of large earthquakes, surrounded by a region of continuing or increasing activity [Kanamori, 1981]. This seismicity pattern has been given the name “Mogi doughnut” [e.g., Mogi, 1969], with the doughnut hole representing the low seismicity rate around the impending hypocenter. However, analyses of large earthquake catalogs to evaluate the reliability of quiescence in predicting earthquakes have yielded mixed results [Habermann, 1988; Reasenberg and Matthews, 1988]. At shorter time scales of days to hours, some earthquakes are preceded by foreshock sequences near their hypocenters, but no distinctive properties in these sequences have yet been identified that would distinguish them from the many observations of earthquake clusters that do not lead to large earthquakes.

[3] Recently, considerable attention has focused on the statistics of earthquake triggering, in which the occurrence of an earthquake increases the probability of a subsequent nearby event, and models have been derived with a single unified triggering law, which can explain the general properties of earthquake catalogs, including foreshock and aftershock sequences [e.g., Ogata, 1999; Helmstetter and Sornette, 2002]. In many of these models [e.g., Helmstetter and Sornette, 2003; Felzer et al., 2004], prior seismicity increases the probability of a future earthquake in the same region but does not change the size distribution of the triggered events, which is governed by the Gutenberg-Richter magnitude-frequency relation, a power law that produces many more small earthquakes than large earthquakes. These models predict no difference in the average seismicity prior to earthquakes of any specified size. There are many more M 4 earthquakes than M 7 earthquakes, but there should be no resolvable differences in the average rate or spatial distribution of seismicity prior to any individual earthquakes of any size. These models therefore contradict the hypothesis that Mogi doughnuts and quiescence are distinctive precursory phenomena for large earthquakes.

[4] Resolving between these competing models is important because it touches on questions regarding the predictability of earthquakes. If Mogi doughnuts and/or quiescence can be reliably established, this would imply at least some differences in the stress distribution or crustal properties prior to large earthquakes. However, if observations show that average precursory seismicity is identical between large and small events, then larger earthquakes likely represent the essentially random occurrence of rare events in a power law distribution of event sizes (perhaps representing a runaway cascade of rupture initiated by a smaller earthquake) and will be very difficult to predict. Testing these models for large earthquakes is challenging because of the limited number of these earthquakes in the available catalogs. However, recent advances in the location accuracy of small earthquakes suggest that it may be possible to search

¹Institute of Geophysics and Planetary Physics, University of California, San Diego, La Jolla, California, USA.

²Department of Geology and Geophysics, University of Wisconsin–Madison, Madison, Wisconsin, USA.

³Now at Division of Marine Geology and Geophysics, Rosenstiel School of Marine and Atmospheric Science, University of Miami, Miami, Florida, USA.

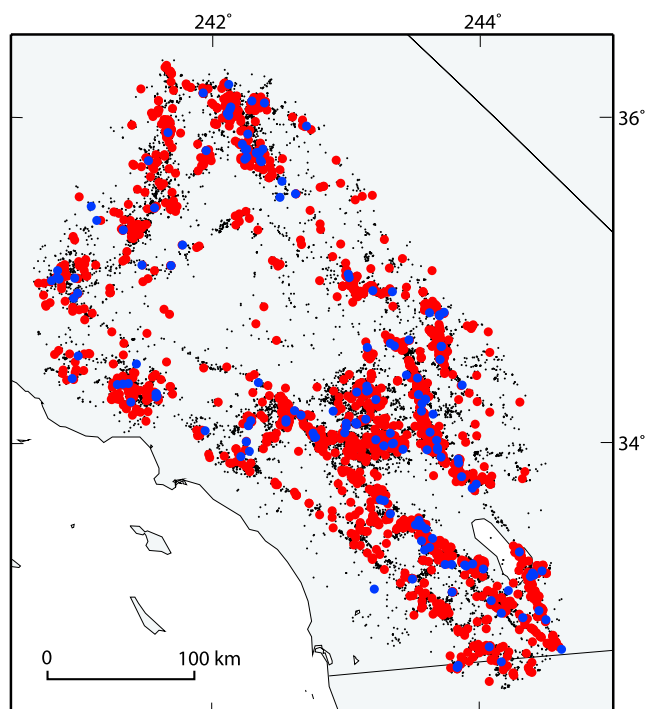


Figure 1. Targeted earthquakes in the LSH catalog of southern California seismicity. $M \geq 2$ events are shown as small black dots, $M \geq 3$ as red dots, and $M \geq 4$ as blue dots. $M \geq 5$ events are not plotted.

for Mogi-like behavior on smaller and more numerous events, thus obtaining more reliable statistics regarding possible precursory behavior. Here we document regions of enhanced activity in 1-day periods preceding moderate sized earthquakes (M 2 to 5) in southern California at distances comparable to their predicted source radii.

2. Analysis of Southern California Seismicity

[5] We analyze precursory seismicity in a recent catalog [Lin *et al.*, 2007] for southern California computed using waveform cross correlation, which provides relative location accuracy of 100 m or less among nearby events. Lin *et al.*'s catalog (named LSH) spans 1981 to 2005 and includes 433,166 events over a magnitude range from less than 1 to over 7. To obtain a more uniform data set, we window the catalog to include only events of $M \geq 1.5$ that are located inside the network and identified as local earthquakes by the network operators (i.e., excluding quarry blasts), reducing the catalog to 173,058 events. We sum and average seismic activity prior to target events in three bins at unit magnitude intervals between M 2 and 5. Because catalog completeness often suffers following major earthquakes owing to the high seismicity rate [e.g., Kagan, 2004], we do not include target events during certain specified time periods. Specifically, we exclude target earthquakes for 1 month following the 1987 M 6.2/6.6 Elmore Ranch/Superstition Hills and 1992 M 6.1 Joshua Tree earthquakes, 2 months following the 1994 M 6.7 Northridge earthquake, and 3 months following the 1992 M 7.3 Landers and 1999 M 7.1 Hector Mine earthquakes. We also exclude target events if they follow an event of $M \geq 4$ within 3 days and 150 km. Our intention is not to remove all aftershocks or to “decluster” the data, but

simply to exclude time periods when it is likely that events are less completely cataloged. For the LSH catalog, this results in 35,391 M 2–3 target events, 2075 M 3–4 events, and 162 M 4–5 events (see Figure 1).

[6] Earthquakes prior to the target events are summed in 100 space-time bins, evenly spaced in 10 log distance bins between 0.01 and 100 km and in 10 log time bins from 0.001 to 1000 days. We count all precursory earthquakes, not just those that are smaller than the target events. Figure 2a contours the resulting estimates of average precursory event density as a function of time before and distance from the target events in the LSH catalog (see Appendix A for additional details of the construction of Figure 2). We do not attempt to correct for edge effects at large distances caused by the free surface, the ~ 20 km maximum event depth, and our geographic window. The results for the M 2–3 target earthquakes are smoothest because of the much larger number of events. The event density is greatest at small times and distances, reflecting the strong space-time clustering of the seismicity. At short times, the nearly evenly spaced contours in log event rate indicate a power law distribution, which has been previously observed and often is related to a fractal dimension for the seismicity. However, Figure 2a makes clear that seismicity is clustered in time as well as space and that computed fractal dimensions will vary depending upon the time interval that is considered, as noted by Kagan [2007].

[7] Comparing plots of this type showing average seismicity rates both before and after the target events could be used to address the question of how much the space-time clustering of seismicity is caused by earthquake-to-earthquake triggering [e.g., Felzer and Brodsky, 2006], as opposed to an underlying physical process. However, our emphasis in this study is on examining possible differences in precursory activity among earthquakes of different sizes, which can be considered independently of the process causing the clustering as well as edge effects arising from the finite size of our catalog. Our results also do not require catalog completeness or aftershock removal, provided catalog properties do not vary systematically prior to earthquakes of different sizes.

[8] Average precursory event rates for the M 3–4 and M 4–5 bins (Figures 2b and 2c) are grossly similar to the M 2–3 bin but are more irregular and less complete owing to the smaller number of target events available for averaging. Figures 2d and 2e show the ratio of precursory seismicity rates for the larger magnitude bins compared to rates for the M 2–3 bins. These results exhibit considerable variation but the clearest anomaly is a 30% to 100% increase in the precursory seismicity rate for the larger events (compared to the M 2–3 events) at distances between 0.3 and 5 km from their eventual hypocenters. The seismicity increase is most pronounced in the 1-day period preceding the earthquakes. To see this anomaly more clearly, Figure 3 plots results for this 1-day period for (Figure 3a) linear event rate (events per day per kilometer from source, rather than normalized by volume as in Figure 2), (Figure 3b) the increase or decrease in the average number of precursory events for larger magnitude earthquakes compared to the M 2–3 events, and (Figure 3c) the cumulative number of extra or missing events (i.e., integrating Figure 3b over distance). An increase in seis-

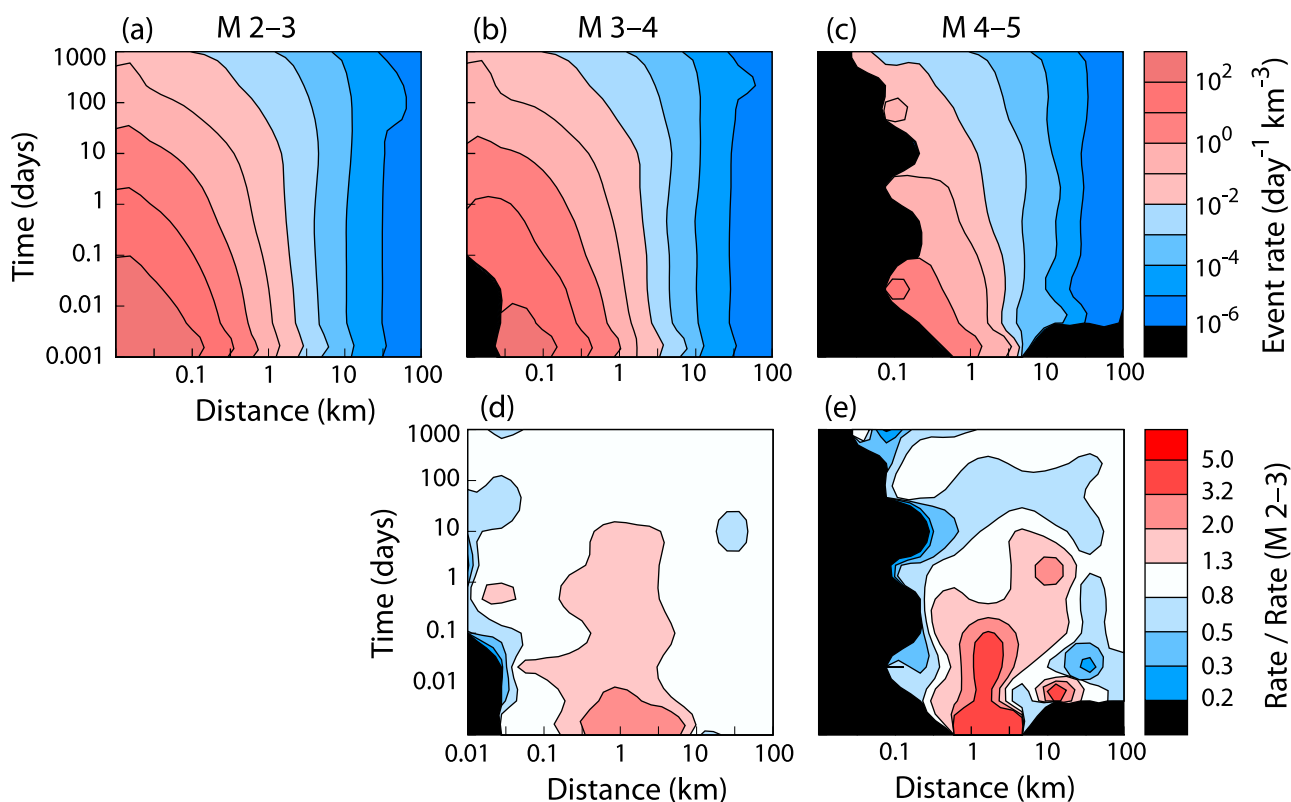


Figure 2. Space/time behavior of precursory seismicity in southern California. (top) The average event rate prior to target earthquakes of (a) M 2–3, (b) M 3–4, and (c) M 4–5, at times from 0.001 day (86 s) to 1000 days prior to the target events at distances from 10 m to 100 km. Contours are uniform in log event density (per day per cubic kilometer). Black shows regions of no data. (bottom) The ratio of precursory seismicity rate for the (d) M 3–4 and (e) M 4–5 target event bins compared to the M 2–3 bins.

micity rate for the larger earthquakes is apparent between about 0.2 and 5 km. A bootstrap resampling approach [e.g., Efron and Tibshirani, 1991] is used to estimate standard error bars, in which we randomly resample the target event population 1000 times and then obtain standard errors from the distribution of results obtained within each bin. See Appendix A for additional details regarding the construction of Figure 3.

[9] The seismicity increase is more pronounced and peaks at a larger distance for the M 4–5 target earthquakes than the M 3–4 earthquakes. However, the increase is more statistically significant for the M 3–4 targets than the M 4–5 targets as shown by the error bars in Figure 3, which indicate that the anomaly exceeds two standard errors for three of the distance bins. In contrast, the M 4–5 increased seismicity anomaly exceeds one standard error in four distance bins, but only approaches two standard errors in one of the bins. For this bin, there is roughly a 2.5% probability that the increased seismicity occurred by chance.

[10] There is also a deficit of precursory events for the larger target earthquakes at short distances, which is most apparent for the M 3–4 results at distances less than 60 m and for the M 4–5 results at distances less than 300 m. As shown by the error bars in Figure 3, this precursory quiescence at short distances is more statistically significant for the M 4–5 earthquakes than the seismicity increase at longer distances. No results are shown for M 4–5 precursory event densities at the two closest distance bins (i.e., 10–25 m and 25–63 m) because there are no events to

count. To estimate the statistical significance of the absence of M 4–5 precursors at these distances, we performed a bootstrap test in which we randomly picked 162 events (the number of M 4–5 target events) from the 35,391 M 2–3 target events. We obtained zero events in the 10–25 m bin 85% of the time and zero events in the 25–63 m bin 35% of the time. Thus, no significance should be assigned to the lack of M 4–5 precursors at these distances. However, a similar test indicated that the decreased precursory event density for the M 4–5 targets compared to the M 2–3 targets is statistically significant (exceeding two standard errors) for both the 63–159 m and 159–398 m bins. Similarly, we tested the significance of the deficit of M 3–4 precursors at close distances by randomly picking 2075 events (the number of M 3–4 target events) from the 35,391 M 2–3 target events and found that the deficit at the closest distance bin (10–25 m) exceeds two standard errors but that the deficit at the 25–63 m bin only exceeds one standard error in significance. Finally, we used this approach (i.e., sampling reduced numbers of M 2–3 target quakes) to test the significance of the increased seismicity for the M 3–4 and M 4–5 targets at distances near 1 km, and generally found results in agreement with the error bars plotted in Figure 2, that is, that the M 3–4 increases are clearly significant, but that the M 4–5 increases are only significant at the one standard error level.

[11] The increase in precursory seismicity occurs at distances that roughly correspond to the expected source radius of the target earthquakes, which is 200 m for M_w 3 earth-

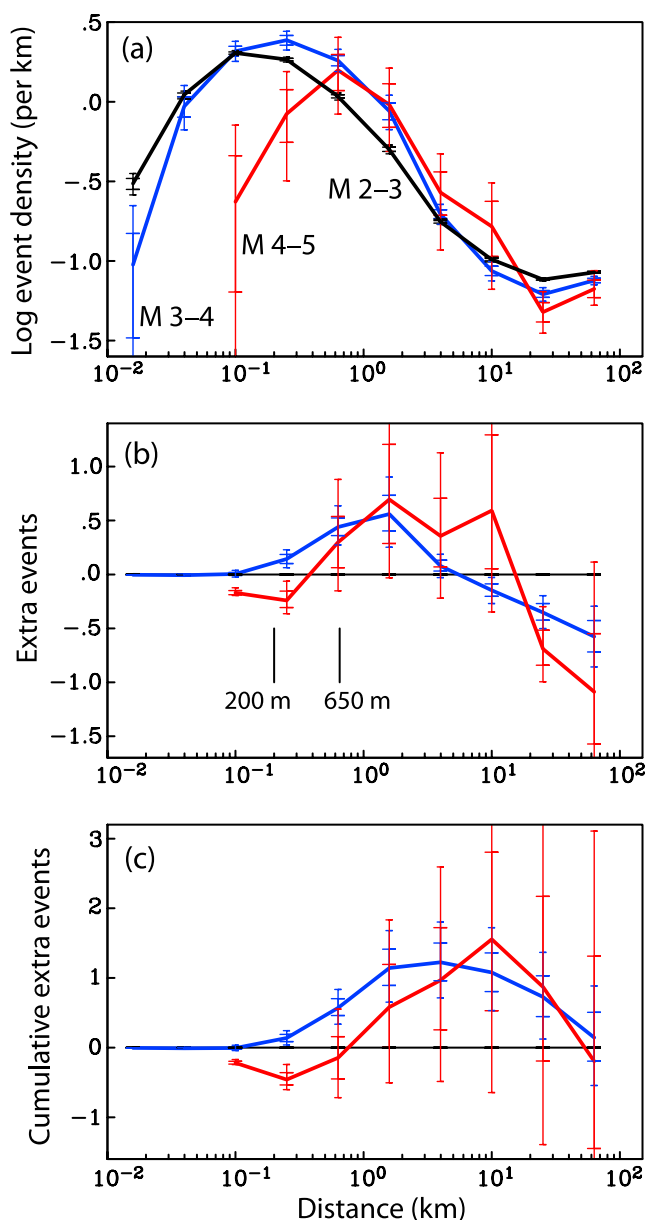


Figure 3. Average seismicity during the day prior to earthquakes of different sizes, plotted versus distance. Results for target events of M 2–3, 3–4 and 4–5 are shown as black, blue, and red lines, respectively, with one and two standard error bars. (a) Linear event density, (b) extra events in each distance bin compared to the M 2–3 results, and (c) distance integrated extra events, i.e., the number of extra events within each maximum distance.

quakes and 650 m for M_w 4 earthquakes, assuming a circular crack model and a 2 MPa stress drop (the median stress drop observed by *Shearer et al.* [2006] for small earthquakes in southern California).

3. Robustness of Results

[12] Because these observed precursory patterns are subtle and apparent only after stacking large numbers of events, it is important to test whether they are a robust result and not some kind of artifact. Here we check the sensitivity of our

results with respect to a number of our data processing choices, including our contouring method, our cutoff magnitude, our excluded time periods, and the earthquake catalog itself.

[13] Figure 4 is similar to Figure 2, but plots the original (uncontoured) values in each of the 10 by 10 bins. This demonstrates that the enhanced precursory activity is not an artifact of the contouring method. We prefer to show the contoured results because it is easier to see the overall space/time dependence of the seismicity rate in Figures 2a–2c.

[14] Earthquake catalogs miss some fraction of smaller earthquakes and are said to be “complete” only above some threshold magnitude. It is unlikely that the LSH catalog is complete down to M 2, even within the restricted region that we study. However, because we focus exclusively on the issue of whether systematic differences exist in the precursory seismicity prior to small to moderate earthquakes, our results do not require overall catalog completeness, provided the catalog properties are reasonably uniform with time. Nonetheless it would be troubling if our results varied substantially as a function of the cutoff magnitude that we apply. Figures 5a and 5b show results for $M \geq 1$ and $M \geq 2$, respectively, and should be compared with the results in Figures 2 and 3 for $M \geq 1.5$. Although there are some variations, the main results are unchanged.

[15] We exclude target events for specified time periods following moderate to large earthquakes not because aftershocks are intrinsically unsuitable as target events but because catalog completeness is known to suffer during times of high aftershock activity. We make no attempt to remove all aftershocks or to “decluster” the data, nor would that necessarily be desirable because there is often no clear distinction between aftershocks and other events. To test whether our choice of exclusion windows is affecting our results, we repeat our analyses using exclusion windows half as long (Figure 5c) and twice as long (Figure 5d) as those used in the main paper (i.e., scaling both the months long window for $M \geq 6$ quakes and the 3-day window for $M \geq 4$ quakes). The overall position and sizes of the precursory anomalies are robust with respect to these changes.

[16] Because all events of $M \geq 4$ in the LSH catalog were located without waveform cross correlation, unlike many of the smaller event locations, we also repeated our analyses using a catalog in which all events were relocated in the same way (source-specific station terms and a 3-D velocity model, no waveform cross-correlation; for details, see *Lin et al.* [2007]). These results (shown in Figure 5e) are similar to those for the LSH catalog at distances beyond about 1 km, but the deficit of precursory earthquakes at short distances for the larger target events disappears, presumably as a result of increased location errors. This highlights that our observed deficit of precursory earthquakes at short distances depends upon the accuracy of the locations achieved using waveform cross-correlation methods. The observed surplus of events at 0.5 to 5 km distance does not require the same degree of location accuracy.

4. Discussion

[17] The reliability of the results presented here depends upon the relative location accuracy among the events in the

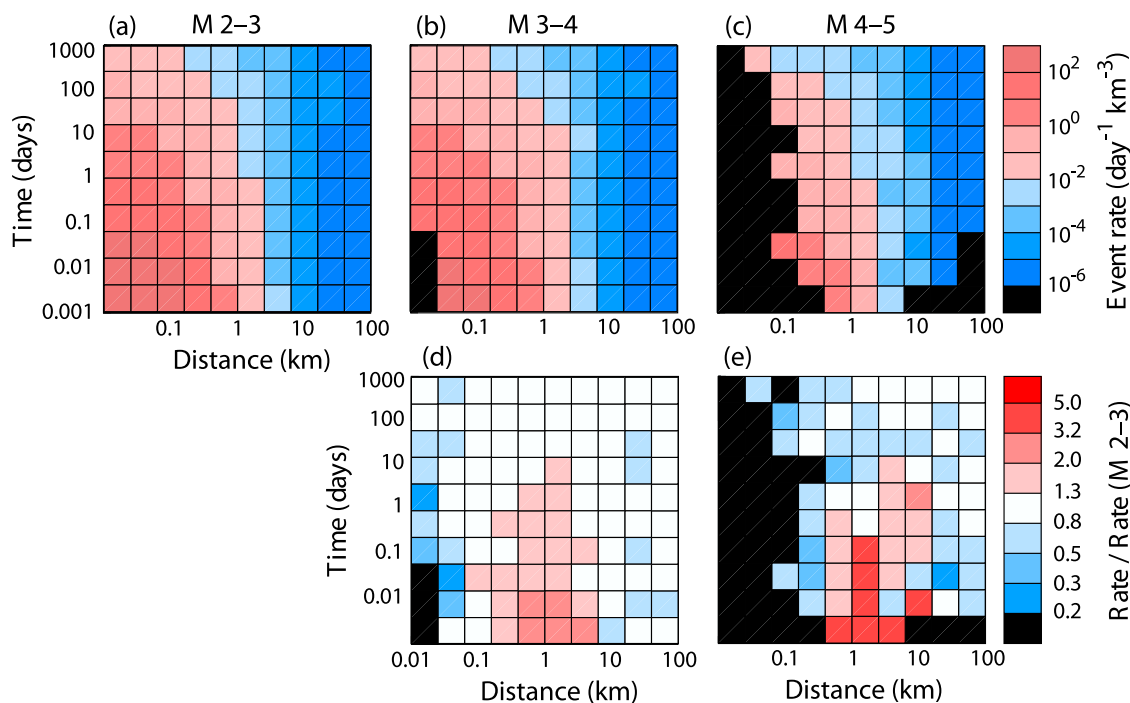


Figure 4. Space/time behavior of precursory seismicity in southern California. (top) The average event rate prior to target earthquakes of (a) M 2–3, (b) M 3–4, and (c) M 4–5, at times from 0.001 day (86 s) to 1000 days prior to the target events at distances from 10 m to 100 km. Black shows cells with no data. (bottom) The ratio of precursory seismicity rates for the (d) M 3–4 and (e) M 4–5 target event bins compared to the M 2–3 bin.

underlying earthquake catalog. A potential source of bias would exist if the quality of the locations were magnitude-dependent. In particular, if the larger magnitude events were less accurately located, this might shift them away from their true locations within dense seismicity and potentially mimic the Mogi doughnut pattern that we see. This scenario could occur for larger events in high-resolution catalogs based on waveform cross correlation because often larger events do not cross correlate as well with neighboring events as do smaller events and thus their relative locations are less reliably resolved. However, the size of the location errors for larger events would not necessarily be expected to match the predicted source radii of the events. In addition, an error in the target event location should not affect the cumulative number of earthquakes at large distances. Figure 3c shows that the cumulative number of earthquakes for the three magnitude bins converge at about 100 km distance, much greater than any possible event location error. A related issue is that for larger events the hypocenter may be different from the centroid of moment release. It is not clear if the seismicity “hole” that we observe is more centered around the hypocenter or the centroid. However, resolving this will be difficult because there are very few finite source models for M 3–5 earthquakes.

[18] Catalog completeness is an important issue in statistical studies of seismicity. Our results do not depend upon overall catalog completeness, but might be biased if the larger magnitude target events were cataloged more completely during periods of high seismicity than smaller

magnitude events. We have attempted to reduce this possibility by spatially windowing the catalog to its best resolved part, using target events only of M 2 and greater, and avoiding target events immediately following large earthquakes. In any case it would be difficult for this bias to mimic the behavior that we observe of increased precursory seismicity concentrated in a 1-day period 0.2 to 5 km away from the target events. Catalog completeness is less important for the precursory events themselves (because we are making only relative comparisons between results for the different target event sizes), but we have verified that we obtain similar results for magnitude cutoffs of M 1, M 1.5, and M 2 (see section 3).

[19] It should be emphasized that these magnitude-dependent differences in the precursory behavior of California earthquakes are apparent only after averaging over hundreds to thousands of earthquakes. Although the 1-day precursory seismicity rate increases by 30% to 100% for the M 3–4 and M 4–5 quakes compared to the M 2–3 quakes (at about 1 km distance), this corresponds, on average, to only about one extra precursory event per target event, because of the overall low rate of precursory activity. Thus, these results are not useful for devising prediction schemes for individual M 4 earthquakes. Rather, their importance is that they imply a failure of the hypothesis in many earthquake triggering models that large earthquakes have precursory seismicity identical to small earthquakes. The fact that the distance to the region of enhanced seismicity seems to roughly scale with the radii of the ensuing earthquakes supports the idea that stress release may concentrate at the

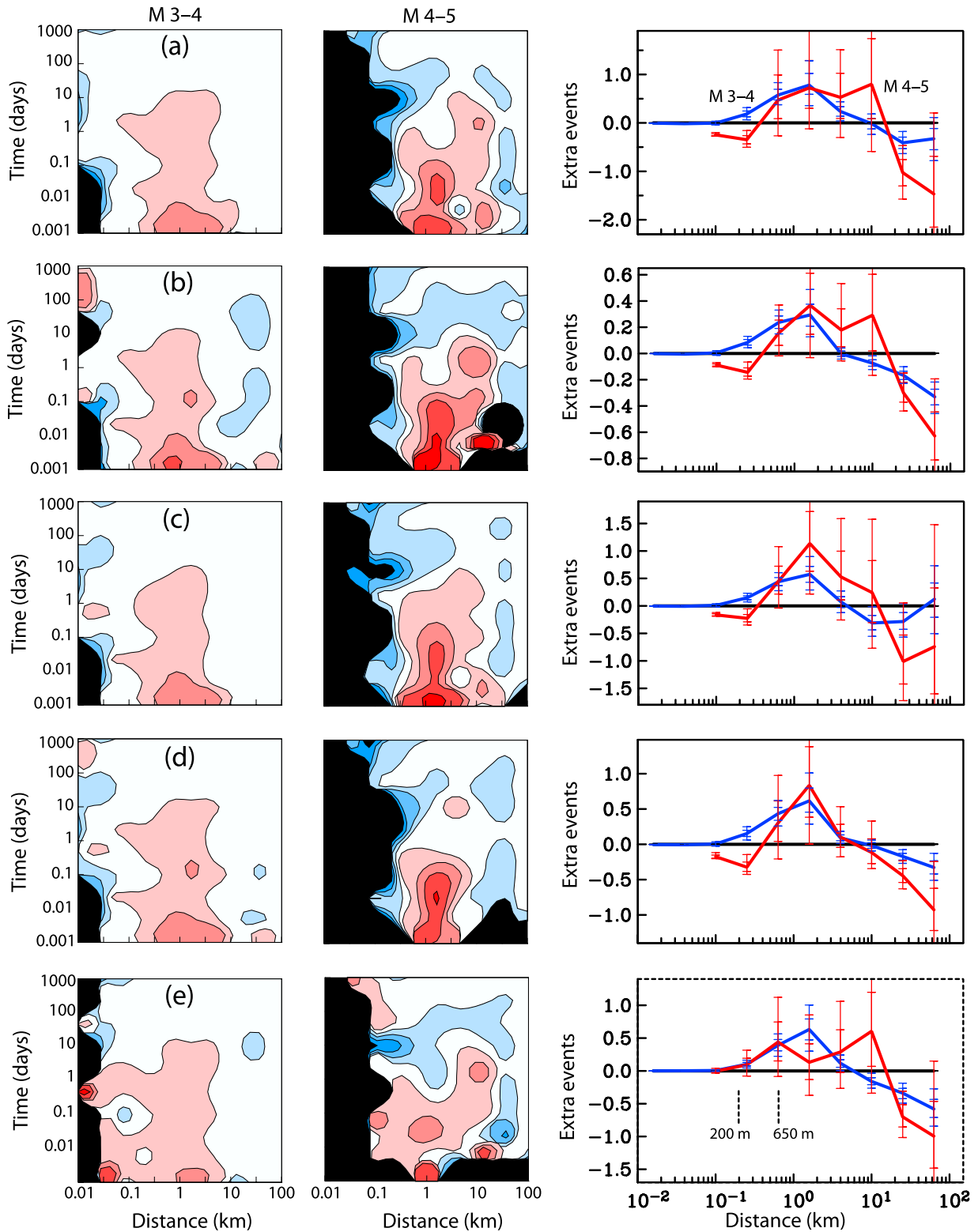


Figure 5. Results for (a) minimum event magnitude of 1.0 and (b) minimum event magnitude of 2.0, (c) halved aftershock exclusion periods, (d) doubled aftershock exclusion periods, and (e) SSST only earthquake catalog. (left and middle) Correspond to Figures 2d and 2e and (right) corresponds to Figure 3b.

edges of the eventual rupture zone. But these effects are subtle and occur clearly only within a ~ 1 day interval before the target earthquakes.

[20] Aftershocks are sometimes observed to cluster around the edges of the main shock rupture. *Rubin and Gillard* [2000] observed an absence of aftershocks closer

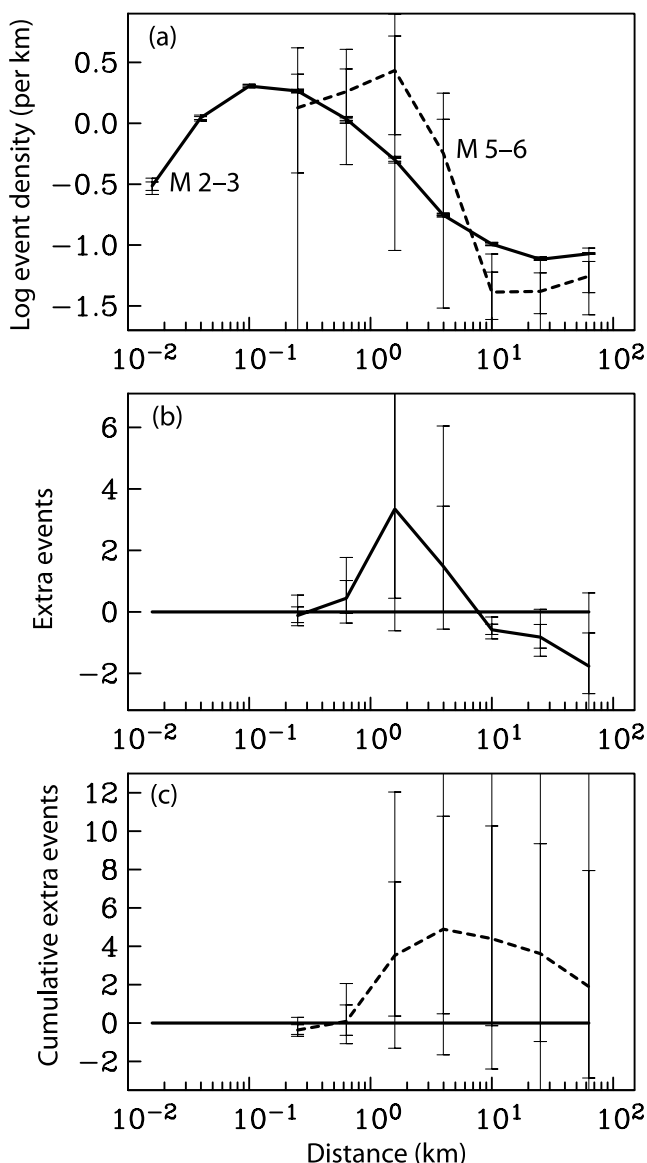


Figure 6. Average seismicity during the day prior to earthquakes of M 5–6 (dashed) compared to those prior to M 2–3 earthquakes (black), plotted versus distance with one and two standard error bars. (a) Linear event density, (b) extra events in each distance bin compared to the M 2–3 results, and (c) distance integrated extra events, i.e., the number of extra events within each maximum distance.

than 10 m to M 1 events and closer than 100 m to an M 3.5 earthquake in central San Andreas Fault seismicity relocated using waveform cross correlation. These distances correspond to those expected for a circular rupture and a 10 MPa stress drop. The significance of our results is that they demonstrate that an analogous phenomenon seems to occur for precursory seismicity, at least for small to moderate sized earthquakes in southern California. However, the cause of this effect is likely different, i.e., the aftershocks may tend to be suppressed in the region where stress has been released by slip on the fault, whereas the precursors

are suppressed within a locked patch near the eventual hypocenter.

[21] It is possible that larger and longer-lasting precursory differences also exist for bigger earthquakes (i.e., $M > 5$), but there are too few of these earthquakes in the LSH catalog to yield statistically reliable results. Figure 6 plots results for 27 target events of M 5–6. Although suggestive of increased precursory seismicity between 500 m and 5 km, the results are barely statistically significant at the one error bar level because of the small number of target earthquakes. There is also no evidence that the number of extra events occurs at greater distance than the M 4–5 target event results (i.e., scaling with the expected M 5 source radius of ~ 2 km).

[22] Some large California earthquakes have been preceded by foreshock sequences [e.g., Dodge *et al.*, 1996], which tend to occur near the main shock hypocenter rather than at the edges of the main shock rupture area. If precursory seismicity anomalies occur for larger earthquakes analogous to our observations for M 3–5 earthquakes, they would be at greater distances from the hypocenter than most documented foreshock observations. However, these more extended anomalies may be hard to resolve if they represent small changes in seismicity rate, owing to the small number of $M > 5$ earthquakes in the available catalogs.

[23] There have been many efforts to identify precursory patterns in seismicity, both in real [e.g., Mogi, 1969; Kanamori, 1981; Habermann, 1988; Reasenberg and Matthews, 1988; Wyss *et al.*, 1996; Maeda, 1999; Joswig, 2001] and simulated earthquake catalogs [e.g., Hainzl *et al.*, 2000; Mori and Kawamura, 2005; Kawamura, 2006]. In addition to the Mogi doughnut hypothesis, other ideas have included accelerated moment release [e.g., Bowman *et al.*, 1998; Jaume and Sykes, 1999] and growing correlation length changes [e.g., Zoller *et al.*, 2001; Huc and Main, 2003; Ouillon and Sornette, 2004]. However, the validity of these possible precursors has been questioned because of the limited numbers of events in seismicity catalogs and the possibility that data windowing methods may be biasing the results [Hardebeck *et al.*, 2008]. An advantage of examining smaller earthquakes is that more reliable statistics can be obtained. To the extent that seismicity is a self-similar process, it is likely that behavior seen for small earthquakes also occurs for larger events and may be useful in earthquake forecasting based on the statistics of earthquake clustering [e.g., Kagan and Jackson, 2000; Gerstenberger *et al.*, 2005].

Appendix A

[24] The values plotted in Figures 2 and 3 are computed as follows. Define each space/time bin with minimum and maximum times, t_1 and t_2 , before the target event, and minimum and maximum distances, r_1 and r_2 , from the target event. For each bin, sum the total number of precursory events for all target events. The event rate, D (plotted in Figures 2a–2c), is then given by

$$D = \frac{n}{N(t_2 - t_1)(4/3)\pi(r_2^3 - r_1^3)}, \quad (\text{A1})$$

where n is the total number of precursory events in the space/time bin and N is the number of target events. We do not attempt to correct for edge effects at large distances caused by the free surface, the ~ 20 km maximum event depth, and our geographic window. The relative change in precursory event rate, D_{rel} (plotted in Figures 2d and 2e), in each bin with respect to the results for the M 2–3 bin is expressed as the ratio

$$D_{rel} = D/D_{M\ 2-3}, \quad (A2)$$

where $D_{M\ 2-3}$ is the rate for the M 2–3 target events. The linear event density in the day prior to the target events, D_{lin} (plotted in Figure 3a), in each bin is given by

$$D_{lin} = \frac{n}{N(r_2 - r_1)}. \quad (A3)$$

The average number of extra events, E , in each bin relative to the M 2–3 results is given by

$$E = \frac{n}{N} - \frac{n_{M2-3}}{N_{M2-3}} \quad (A4)$$

and is plotted in Figure 3b. Finally, the cumulative number of extra events (plotted in Figure 3c) is given by

$$E = \frac{m}{N} - \frac{m_{M2-3}}{N_{M2-3}}, \quad (A5)$$

where m is the total number of events within distance r_2 in the 1-day period before each target event.

[25] The bootstrap resampling method is applied to the entire target event population. Each of the 1000 resamples is obtained by randomly repicking the same number of total target events, which typically results in some events being picked more than once and some not at all. Because the total target population is resampled, the number of target events within each magnitude bin will vary randomly. The one- and two-standard error bars for the various parameters in the plots are computed as the 2.5%, 17%, 83%, and 97.5% points in the resulting distributions.

[26] **Acknowledgments.** We thank Duncan Agnew and reviewers David Schaff and Karen Felzer for valuable suggestions. This research was supported by the U.S. Geological Survey (USGS), the National Science Foundation (NSF), and the Southern California Earthquake Center (SCEC). SCEC is funded by NSF Cooperative Agreement EAR-0106924 and USGS Cooperative Agreement 02HQAG0008. This is SCEC contribution 1241.

References

- Bowman, D. D., G. Ouillon, C. G. Sammis, A. Sornette, and D. Sornette (1998), An observational test of the critical earthquake concept, *J. Geophys. Res.*, *103*, 24,359–24,372, doi:10.1029/98JB00792.
- Dodge, D. A., G. C. Beroza, and W. L. Ellsworth (1996), Detailed observations of California foreshock sequences: Implications for the earthquake initiation process, *J. Geophys. Res.*, *101*, 22,371–22,392, doi:10.1029/96JB02269.
- Efron, B., and R. Tibshirani (1991), Statistical data analysis in the computer age, *Science*, *253*, 390–395, doi:10.1126/science.253.5018.390.
- Felzer, K., and E. Brodsky (2006), Decay of aftershock density with distance indicates triggering by dynamic stress, *Nature*, *441*, 735–738, doi:10.1038/nature04799.
- Felzer, K., R. Abercrombie, and G. Ekstrom (2004), A common origin for aftershocks, foreshocks, and multiplets, *Bull. Seismol. Soc. Am.*, *94*, 88–98, doi:10.1785/0120030069.
- Gerstenberger, M. C., S. Wiemer, L. M. Jones, and P. A. Reasenber (2005), Real-time forecasts of tomorrow's earthquakes in California, *Nature*, *435*, 328–331, doi:10.1038/nature03622.
- Habermann, R. E. (1988), Precursory seismic quiescence: Past, present, and future, *Pure Appl. Geophys.*, *126*, 279–318, doi:10.1007/BF00879000.
- Hainzl, S. (2004), Seismicity patterns of earthquake swarms due to fluid intrusion and stress triggering, *Geophys. J. Int.*, *159*, 1090–1096, doi:10.1111/j.1365-246X.2004.02463.x.
- Hainzl, S., G. Zöller, J. Kurths, and J. Zschau (2000), Seismic quiescence as an indicator for large earthquakes in a system of self-organized criticality, *Geophys. Res. Lett.*, *27*, 597–600, doi:10.1029/1999GL011000.
- Hardebeck, J. L., K. R. Felzer, and A. J. Michael (2008), Improved tests reveal that the accelerating moment release hypothesis is statistically insignificant, *J. Geophys. Res.*, *113*, B08310, doi:10.1029/2007JB005410.
- Helmstetter, A., and D. Sornette (2002), Diffusion of epicenters of earthquake aftershocks, Omori's law, and generalized continuous-time random walk models, *Phys. Rev. E*, *66*, 061104, 1–24.
- Helmstetter, A., and D. Sornette (2003), Foreshocks explained by cascades of triggered seismicity, *J. Geophys. Res.*, *108*(B10), 2457, doi:10.1029/2003JB002409.
- Huc, M., and I. G. Main (2003), Anomalous stress diffusion in earthquake triggering: Correlation length, time dependence, and directionality, *J. Geophys. Res.*, *108*(B7), 2324, doi:10.1029/2001JB001645.
- Jaume, S. C., and L. R. Sykes (1999), Evolving towards a critical point: A review of accelerating seismic moment/energy release prior to large and great earthquakes, *Pure Appl. Geophys.*, *155*, 279–306, doi:10.1007/s000240050266.
- Joswig, M. (2001), Mapping seismic quiescence in California, *Bull. Seismol. Soc. Am.*, *91*, 64–81, doi:10.1785/0119980160.
- Kagan, Y. Y. (2004), Short-term properties of earthquake catalogs and models of earthquake source, *Bull. Seismol. Soc. Am.*, *94*, 1207–1228, doi:10.1785/012003098.
- Kagan, Y. Y. (2007), Earthquake spatial distribution: The correlation dimension, *Geophys. J. Int.*, *168*, 1175–1194, doi:10.1111/j.1365-246X.2006.03251.x.
- Kagan, Y. Y., and D. Jackson (2000), Probabilistic forecasting of earthquakes, *Geophys. J. Int.*, *143*, 438–453, doi:10.1046/j.1365-246X.2000.01267.x.
- Kanamori, H. (1981), The nature of seismicity patterns before large earthquakes, in *Earthquake Prediction: An International Review*, Maurice Ewing Ser., vol. 4, edited by D. Simpson and P. Richards, pp. 1–19, AGU, Washington, D. C.
- Kawamura, H. (2006), Spatiotemporal correlations of earthquakes, in *Lecture Notes in Physics*, vol. 705, *Modelling Critical and Catastrophic Phenomena in Geoscience*, edited by P. Bhattacharyya and B. K. Chakrabarti, pp. 223–257, Springer, Berlin.
- Lin, G., P. M. Shearer, and E. Hauksson (2007), Applying a three-dimensional velocity model, waveform cross correlation, and cluster analysis to locate southern California seismicity from 1981 to 2005, *J. Geophys. Res.*, *112*, B12309, doi:10.1029/2007JB004986.
- Maeda, K. (1999), Time distribution of intermediate foreshocks obtained by a stacking method, *Pure Appl. Geophys.*, *155*, 381–394, doi:10.1007/s000240050270.
- Mogi, K. (1969), Some features of recent seismic activity in and near Japan (2), Activity before and after great earthquakes, *Bull. Earthquake Res. Inst. Univ. Tokyo*, *47*, 395–417.
- Mori, T., and H. Kawamura (2005), Simulation study of spatiotemporal correlations of earthquakes as a stick-slip frictional instability, *Phys. Rev. Lett.*, *94*, 1–4, 058501.
- Ogata, Y. (1999), Seismicity analysis through point-process modeling: A review, *Pure Appl. Geophys.*, *155*, 471–507, doi:10.1007/s000240050275.
- Ouillon, G., and D. Sornette (2004), Search for direct empirical spatial correlation signatures of the critical triggering earthquake model, *Geophys. J. Int.*, *157*, 1233–1246, doi:10.1111/j.1365-246X.2004.02269.x.
- Reasenber, P., and M. Matthews (1988), Precursory seismic quiescence: A preliminary assessment of the hypothesis, *Pure Appl. Geophys.*, *126*, 373–406, doi:10.1007/BF00879004.
- Rubin, A. M., and D. Gillard (2000), Aftershock asymmetry/rupture directivity among central San Andreas fault microearthquakes, *J. Geophys. Res.*, *105*, 19,095–19,109, doi:10.1029/2000JB900129.
- Shearer, P. M., G. A. Prieto, and E. Hauksson (2006), Comprehensive analysis of earthquake source spectra in southern California, *J. Geophys. Res.*, *111*, B06303, doi:10.1029/2005JB003979.

- Vidale, J. E., and P. M. Shearer (2006), A survey of 71 earthquake bursts across southern California: Exploring the role of pore fluid pressure fluctuations and aseismic slip as drivers, *J. Geophys. Res.*, *111*, B05312, doi:10.1029/2005JB004034.
- Wyss, M., K. Shimazaki, and T. Urabe (1996), Quantitative mapping of a precursory seismic quiescence to the Izu-Oshima 1990(M6.5) earthquake, Japan, *Geophys. J. Int.*, *127*, 735–743, doi:10.1111/j.1365-246X.1996.tb04052.x.
- Zoller, G., S. Hainzl, and J. Kurths (2001), Observation of growing correlation length as an indicator for critical point behavior prior to large earthquakes, *J. Geophys. Res.*, *106*, 2167–2217, doi:10.1029/2000JB900379.
-
- G. Lin, Division of Marine Geology and Geophysics, Rosenstiel School of Marine and Atmospheric Science, University of Miami, Miami, FL 33149, USA.
- P. M. Shearer, Institute of Geophysics and Planetary Physics, University of California, San Diego, IGPP 0225, 9500 Gilman Drive, La Jolla, CA 92093, USA. (pshearer@ucsd.edu)